JOURNAL OF BACTERIOLOGY, Sept. 2001, p. 5180–5186 Vol. 183, No. 17
0021-9193/01/$04.00+0 DOI: 10.1128/JB.183.17.5180–5186.2001

Cytological Evidence for Association of the Ends of the Linear Chromosome in *Streptomyces coelicolor*

MELODY C. YANG AND RICHARD LOSICK*

Department of Molecular and Cellular Biology, Harvard University, Cambridge, Massachusetts 02138

Received 5 March 2001/Accepted 4 June 2001

The chromosome of the filamentous bacterium *Streptomyces coelicolor* is linear, but the genetic map is circular. We present cytological evidence based on the use of fluorescence in situ hybridization showing that the ends of the chromosome frequently colocalize, in agreement with the idea that the ends are held together, effectively forming a circular chromosome. These observations provide a possible explanation for how a linear bacterial chromosome can exhibit a circular genetic map.

With over 500 species recognized to date, *Streptomyces* forms a large genus in the high-GC-content group of gram-positive bacteria. Members of this group of spore-forming, filamentous soil bacteria undergo a complex life cycle characterized by various morphologic stages (5, 6). When grown on solid media, spores germinate and develop into substrate mycelia consisting of multinucleated, long branching filaments with infrequent septa. As the colony matures, filaments termed aerial mycelia project above the colony surface. Spores, each containing a single chromosome, are then formed by synchronized septation in the multinucleated aerial filaments. Most species of *Streptomyces* do not sporulate when they are grown in liquid cultures.

Streptomyces coelicolor A(3)2 is the best-characterized species from a genetic point of view (17). The earliest evidence that the genetic map of *S. coelicolor* is circular came from conjugative mating experiments involving differentially marked strains (13, 14). All later studies, including protoplast fusion experiments (18), supported the circularity of the genetic map unequivocally. Thus, it came as a surprise when the chromosome of the related species *Streptomyces lividans* 66 was suggested to be linear by physical mapping data (23). Later, through the application of pulsed-field gel electrophoresis, both the *S. coelicolor* and *S. lividans* chromosomes were shown to be linear (24). Whereas most experimentally studied bacteria possess a circular genome, a few, including the Lyme disease-causing spirochete *Borrelia burgdorferi* (3, 9), the obligate intracellular bacterium *Coxiella burnetii* (36), and the erythromycin-producing actinomycete *Saccharopolyspora erythraea* (28), have been found to possess linear genomes. *Agrobacterium tumefaciens* possess two chromosomes, one that is linear and one that is circular (1). More prokaryotes are likely to be found to possess linear genomes as the physical maps of more bacterial species become available. Of the prokaryotes known to have linear genomes, only *Streptomyces* has a well-developed genetic system. The discovery of a linear genome exhibiting circular genetic behavior in *Streptomyces* leads to an interesting question: how is a circular genetic map obtained from a linear genome?

The only other known examples of a linear genome exhibiting circular genetic behavior are certain phage genomes such as that of T4 (33), where map circularity results from their circularly permutated and terminally redundant chromosomes. However, circular permutation does not apply to *Streptomyces* since the chromosomes were shown to have constant ends (24). In their study of phage genetics, Stahl and Steinberg (32) noted that a circular genetic map may arise from a linear genome if recombination is restricted to even numbers of crossovers. Wang et al. (34) tested this model by examining the inheritance of telomeres in plasmid-mediated interspecies crosses between *S. coelicolor* and *S. lividans*. The authors demonstrated a strong bias towards even numbers of crossovers during such matings, supporting the applicability of the Stahl and Steinberg model to the *Streptomyces* linear genome.

It is well known that eukaryotic chromosomes can exhibit higher-order organization, but little evidence has been presented as to whether prokaryotic chromosomes exhibit similar properties. Essentially nothing is known about how chromosomes are organized in *Streptomyces*. A simple explanation for the observed circular genetic behavior is that the two ends of the *Streptomyces* linear chromosome are physically held together to form a circle (16, 34). In such a case, even numbers of crossovers, as observed by Wang et al. (34), would be necessary if complete haploid genomes were to emerge from the mating process (32). Here, we use fluorescent in situ hybridization (FISH) to examine the localization of distinct chromosomal regions within the cell. Our results provide the first cytological evidence that the ends of a linear bacterial chromosome colocalize, suggesting that the chromosome adopts a circular configuration.

MATERIALS AND METHODS

FISH probe preparation. FISH probe preparation was performed using a modified procedure based on the protocol described in the work of Jensen and Shapiro (22). Due to the high GC content of the *S. coelicolor* genome, reactions producing long PCR products are difficult to perform. Therefore, two or three separate PCRs were carried out to achieve the desired length for each probe. To prepare the 9.8-kb *oriC* probe, two PCRs were performed using primers MYO173 and -174 and MYO175 and -176 (primer sequences and PCR product sizes are shown in Table 1) using PfuTurbo DNA polymerase (Stratagene). The PCR fragments obtained were then cloned into the pCR2.1-TOPO vector using

* Corresponding author. Mailing address: Department of Molecular and Cellular Biology, Harvard University, 16 Divinity Ave., Cambridge, MA 02138. Phone: (617) 495-4905. Fax: (617) 496-4642. E-mail: losick@mcb.harvard.edu.

TABLE 1. PCR primers, PCR product sizes, and plasmids constructed for the preparation of FISH probes

Probe	Forward or reverse primer[a]	Sequence	Product size (bp)	Plasmid
oriC 1	MYO173	CGA ACG GAA GTC GGC CAG CGA CAG ATG C	5,072	pMYB236
	MYO174	CGC CGT ACC GAA CGA ATT TGC GAA GGG C		
oriC 2	MYO175	CGC CGT ACC GAA CGA ATT TGC GAA GGG C	4,746	pMYB238
	MYO176	CTC CGA GAA GTT GCT CCA ATA CGC GTG G		
TIR 1	MYO258	GCG ACC CTC GTT GAC TCC GGA GTT GTA TG	3,252	pMYB288
	MYO259	CCC TTC GAC CAC ATC ACC GAC TCC TGA C		
TIR 2	MYO260	GCT CAG AAG CGG CGT CAG CTC TTG AGC AC	3,486	pMYB290
	MYO261	TGT GCA CTG GAC GAC GGG GAT GCG CTC AC		
TIR 3	MYO262	GCC TTC CGT CCT TGA CAA AGT GGC GCT G	3,212	pMYB292
	MYO263	CAA CCA AAC CGA ACA CGC CGC CAG CCA C		
LAdj 1	MYO264	GCG GGA CAG AGC ATC TCG GTT GAG ATC G	3,430	pMYB286
	MYO265	GCC AGG GTC CGC AAC GCA CCT TGG AAG		
LAdj 2	MYO254	GCT TCC ATG CCC AGG CCC TTC GTC CTT C	3,416	pMYB282
	MYO255	CGG ATT GGC AGC TGC TCT GAC ACA GCC TC		
LAdj 3	MYO256	TGG AGG CTG TGT CAG AGC AGC TGC CAA TC	3,269	pMYB284
	MYO257	GGT ACC GGT GGT CAT GTC CGG ACG GAA TC		
Ctrl1 1	MYO189	GGT CTT GAG GTT CGT GAG GTG GTC GGT GC	3,141	pMYB242
	MYO190	TCC CAC TTG TCG TGG ATG TCG TCG TCT		
Ctrl1 2	MYO191	GGG AAG ACG ACG ACA TCC ACG ACA AGT GG	3,048	pMYB244
	MYO192	CAA CAC AGG ACG GGA TTC ATG CCC ACA GC		
Ctrl1 3	MYO193	CTG TGG GCA TGA ATC CCG TCC TGT GTT GG	3,320	pMYB246
	MYO194	GAT CGC CGT CGG CGT TGA ACC TTG TCA GG		
Ctrl2 1	MYO240	GCC GTT GTA CGT CAG TAG ACG AGT TCT TC	3,350	pMYB270
	MYO271	CGG ACA GTA CTC TTC GAC CCG TAC ATC AC		
Ctrl2 2	MYO242	GGG TGA TGT ACG GGT CGA AGA GTA CTG TC	3,589	pMYB272
	MYO243	GAA CGC TTC CCT GCG TTC GTG GTC TGA G		
Ctrl2 3	MYO244	CCA GAA GCC CTA CAC CTC AGA CCA CGA AC	3,142	pMYB274
	MYO245	CCC AAG GCG ACC ACA TGT CCT CAC TGC TG		

[a] The forward primer is listed first.

a TOPO TA cloning kit (Invitrogen) according to the manufacturer's instructions, producing pMYB236 and pMYB238. Five micrograms of each plasmid DNA was combined and digested with 10 U of three frequently cutting restriction enzymes (*Alu*I, *Ban*I, and *Sau*3AI) overnight to obtain fragment sizes ranging from 75 to 150 bp. The DNA was purified by phenol-chloroform extraction, concentrated by ethanol precipitation, and resuspended in 20 μl of a solution containing 10 mM Tris-HCl (pH 8.0) and 0.1 mM EDTA. DNA was denatured by incubation at 94°C for 5 min, immediately placed on ice, and then labeled with modified nucleotide FluoroLink Cy3-dCTP (Amersham) by an oligonucleotide tailing method. A reaction using a mixture containing 135 μM dCTP, 67.5 μM Cy3-dCTP, and 60 U of terminal deoxynucleotide transferase (TdT) in 1× TdT buffer (Promega) was carried out for 2 h at 37°C. The same reaction was carried out for probes labeled with digoxigenin-11-2′-dUTP (Roche Molecular Biochemicals) except that 180 μM dCTP and 20 μM digoxigenin-11-2′-dUTP were used. Proteins and free nucleotides were then removed using a QIAquick nucleotide removal kit (Qiagen) according to the manufacturer's instructions, followed by concentration by ethanol precipitation. The DNA pellet was then resuspended in a suitable volume of TE (10 mM Tris-HCl [pH 8.0], 1 mM EDTA) to give a probe concentration of 200 ng/μl. Labeled probes can be stored at −20°C for 2 to 4 weeks without detectable loss in labeling efficiency. The same method was used for the preparation of the TIR, LAdj, Ctrl1, and Ctrl2 probes except that different primers were used (Table 1).

FISH procedure. *S. coelicolor* strain J1508 (*hisA1 uraA1 strA1 pglNF, SCP2* negative [21]) was used in all FISH experiments because of the low level of fluorescence emitted by this strain (31). Liquid yeast extract-malt extract (YEME) medium (25 ml) supplemented with 50 μg of histidine per ml and 7.5 μg of uracil per ml (19) was inoculated with 50 μl of an *S. coelicolor* J1508 spore suspension and incubated at 30°C with vigorous shaking for 40 to 45 h (optical density at 600 nm, ~0.7). Formaldehyde was added directly to the culture to a final concentration of 3.7% (vol/vol), and cells were fixed at room temperature for 45 min. Cells were harvested by centrifugation at 3,000 × *g* for 10 min at room temperature and washed three times in an equal volume of phosphate-buffered saline (PBS; 140 mM NaCl, 3 mM KCl, 8 mM Na_2HPO_4, 1.5 mM KH_2PO_4 [pH 7.4]). Cells were resuspended in 2.5 ml of PBS and used immediately or stored at 4°C overnight for use the next day.

One milliliter of cells was spun down, resuspended in 1 ml of GTE (50 mM glucose, 20 mM Tris-HCl [pH 7.5], 10 mM EDTA) and divided into five tubes. To each tube, lysozyme stock solution and GTE buffer were added to give a final concentration of 0.625, 1.25, 2.5, 5, or 10 mg of lysozyme per ml, and the tubes were incubated at room temperature for 10 min. Multiple lysozyme concentrations were used due to the observed variability in the optimal lysozyme concentration needed from experiment to experiment. Cells were then washed three times with 1 ml of GTE, spun down in a microcentrifuge at 2,000 × *g* for 2 min each time to collect the cells, and resuspended in 1 to 5 ml of GTE to give an optimal cell density. A 15-well multitest slide (ICN) was coated with poly-L-lysine by adding a drop of a 0.1% (wt/vol) poly-L-lysine solution (Sigma) into each well, left untouched for 2 min, washed with water, and then air dried completely. Ten microliters of cells from each lysozyme treatment was then pipetted into a well

and incubated for 10 min at room temperature. Excess cells were removed by aspiration, and a drop of GTE was added to each well, followed by aspiration to remove loose cells. Dehydration, prehybridization, hybridization, and subsequent wash steps were performed according to the method described in the work of Jensen and Shapiro (22). For slides containing only fluorescent-nucleotide-labeled probes, the slides were mounted in ProLong Antifade (Molecular Probes) according to the manufacturer's instructions. For slides containing digoxigenin-labeled probes, blocking buffer (2% bovine serum albumin in PBS) was added to each well and the slides were incubated for 15 min at room temperature. The blocking buffer was then replaced with 2 μg of anti-digoxigenin-fluorescein Fab fragments (Roche Biochemicals) per ml in blocking buffer and incubated for 2 h at room temperature in a humidifying chamber. After antibody binding, the slide was washed twice in PBS for 5 min each time at room temperature. The slide was then mounted in ProLong Antifade as described above.

For slide observation and fluorescent-micrograph preparation, we used an Olympus BX60 microscope equipped with a MicroMax cooled-charge-coupled-device camera (Princeton Instruments) connected to an IBM personal computer running MetaMorph software version 3.0 (Universal Imaging). A UPlan Fluorite phase-contrast 100× objective was used for both slide observation and photography. A 2-s exposure was used for the collection of fluorescent images, except when DAPI (4′,6′-diamidino-2-phenylindole) was used, in which case a 0.05-s exposure was used. For the bright-field images, a 0.05-s exposure was used. Adobe Photoshop 5.0 was used for all image manipulation.

Coincident-frequency determination. The coincident frequencies for the two types of signals in double-label FISH experiments were determined as follows. To avoid bias, the fluorescent micrographs obtained for the different probes were analyzed independently. Using Adobe Photoshop 5.0, a circle with a 0.46-μm diameter was generated and manually placed on top of each fluorescent focus centered around the central position. The images of the painted circles thus generated, representing the locations of the fluorescent foci from the different channels, were then overlaid. If the two types of painted circles overlapped, they were considered coincident, and if they did not, they were considered separate. The coincident frequency is defined as the fraction of one type of circle generated from one channel overlapping that from the other channel.

Expected coincident frequency for randomly distributed foci. To calculate the expected coincident frequency if *oriC* and LAdj signals were to randomly distribute in cells, the total cellular area and the total coincident area for each type of foci from eight different fields of cells from a dual-label FISH experiment involving the *oriC* and the LAdj probes were determined using the program MetaMorph 3.0. The coincident area for a single focus was defined as the area (in pixels) occupied by a circle with a 0.92-μm diameter. The total coincident area for the *oriC* signals then equals the total number of *oriC* foci observed in all eight fields of cells multiplied by the coincident area. The probability that a randomly distributed LAdj focus would be found coincident with a randomly distributed *oriC* focus would then be the total coincident area (*oriC*) divided by the total cellular area. Similarly, the probability that a randomly distributed *oriC* focus would be found coincident with a randomly distributed LAdj focus would then be the total coincident area (LAdj) divided by the total cellular area.

RESULTS

Strategy. To investigate whether the ends of the *S. coelicolor* chromosome are held together, we performed FISH experiments to look directly at the relative locations of various chromosomal regions within the cell. The *S. coelicolor* chromosome is a linear molecule 8 Mb in length with a centrally located origin of replication (25). The ends of the chromosome consist of long terminal inverted repeats (TIRs) 27.5 kb in length (http://www.sanger.ac.uk/Projects/S_coelicolor/). DNA sequence available from the *S. coelicolor* genome project revealed the precise junctions between the TIRs and the adjacent nonrepeated regions. Accordingly, we designed three hybridization probes corresponding to (i) the origin of replication region, (ii) an internal portion of the TIR located 10 bp from the TIR junction, and (iii) a nonrepeated region close to, but outside of, the left TIR located 163 bp from the TIR junction. We refer to these probes as the *oriC*, TIR, and LAdj probes, respectively (Fig. 1). All probes were approximately 10 kb in length.

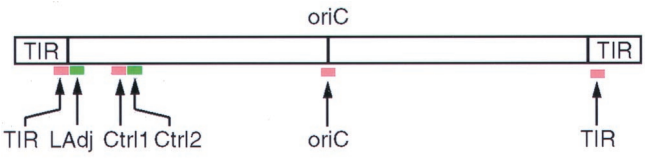

FIG. 1. The positions of FISH probes on the *S. coelicolor* chromosome. The replication origin (*oriC*) is located at the center of the 8-Mb linear chromosome. Identical sequences (27.5 kb in length) named TIRs are found at both ends of the chromosome. The locations of the *oriC*, TIR, LAdj, Ctrl1, and Ctrl2 probes are marked with arrows below the chromosome. The physical distance between LAdj and TIR is 173 bp, and that between Ctrl1 and Ctrl2 is 40 bp. Distances shown are not to scale.

Dual-label FISH experiments involving the TIR and the LAdj probes make distinct predictions depending upon whether the ends of the *S. coelicolor* chromosome are held together. If the two ends of the chromosome are held together, there should be equal numbers of TIR and LAdj signals. Also, a high proportion of TIR signals should be located at or near an LAdj signal. On the other hand, if the two ends of the chromosome are not held together, there should be twice as many TIR signals as LAdj signals. In addition, half of the TIR signals should have a random location within the cell relative to the location of LAdj signals. As a control, a dual-label FISH experiment visualizing two distantly located regions of the chromosome (*oriC* and LAdj) was expected to show no significant association of the two signals.

Separately visualizing *oriC*, TIR, and LAdj. We first determined the subcellular localizations of the *oriC*, TIR, and LAdj regions individually in single-label FISH experiments. Vegetatively growing cells from a liquid culture of *S. coelicolor* were fixed and separately hybridized with the three probes. All three regions of the chromosome appeared as distinct fluorescent foci distributed along the length of the multinucleoid filaments (Fig. 2). In unicellular bacteria the replication origin region preferentially localizes near the cell poles and the terminus near the midcell (10, 26, 35). In contrast, we observed no readily recognizable pattern of focus distribution along the length of the *S. coelicolor* filaments with any of the probes. In *S. coelicolor*, cell wall growth occurs mostly in the mycelial tips (11, 31), raising the possibility that the tip region represents the major site of DNA replication. If so, the mycelial tip regions might be expected to exhibit a different chromosome organization than the nontip regions. However, we observed no difference among the distributions of *oriC* foci at the tips (Fig. 2C and D), the branches (Fig. 2B), and the rest of the mycelium (Fig. 2A). Twin *oriC* spots (bilobed *oriC* foci or two *oriC* foci closely juxtaposed) (Fig. 2A and D) were found in both the tip and the nontip regions and exhibited no preferential distribution to the mycelial tips.

Detection efficiency of the FISH procedure. To determine the staining efficiencies of our FISH probes, we constructed two probes, Ctrl1 and Ctrl2, shown in Fig. 1. Because these two probes hybridize to two regions of the chromosome immediately adjacent to each other, the two signals were expected to colocalize 100% of the time in a dual-label FISH experiment. The staining efficiencies of the probes were then determined by looking at the observed coincidence frequencies (data not

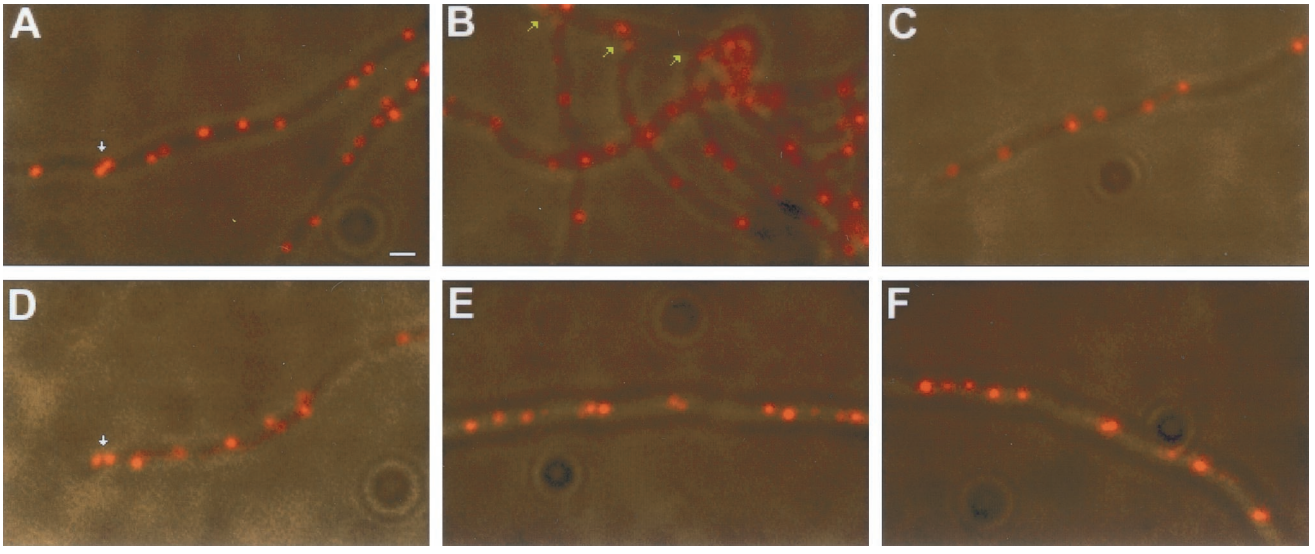

FIG. 2. Single-label FISH experiments showing the subcellular localizations of three chromosomal loci. Cy3-labeled *oriC* and TIR probes and the digoxigenin-labeled LAdj probe were used to detect the subcellular localizations of the replication origin region (A to D), the chromosome ends (E), and a nonrepeated region adjacent to the left TIR (F) in *S. coelicolor* substrate mycelia. (A) Internal portion of the mycelium. (B) Branch region of the mycelium. Green arrows point to branch regions. (C and D) Mycelial tips. White arrows point to twin *oriC* spots. Scale bar = 1 μm.

shown, determined by the method illustrated in Fig. 4 and described below). The Cy3-labeled probe and digoxigenin-labeled probe were found to have 90 and 94% staining efficiencies, respectively.

Dual-label FISH experiments. To determine whether the ends of the chromosomes were located in close proximity to each other, fixed cells from a liquid culture of *S. coelicolor* were hybridized with both a TIR probe and an LAdj probe. As shown in Fig. 3A to D, approximately equal numbers of TIR and LAdj signals were observed and most of the TIR signals were close to or coincident with an LAdj signal. For comparison, a dual-label FISH experiment involving the *oriC* probe and the LAdj probe showed little colocalization of the two fluorescent signals (Fig. 3E to H). Taken together, our data demonstrate that the terminal regions of the chromosome, which are 8 Mb apart, colocalize but that regions of the chromosome (*oriC* and LAdj) that are separated by 4 Mb do not. These conclusions were confirmed quantitatively as follows. One complication in our analysis was variability in the size of FISH signals, which ranged from 0.26 to 0.59 μm in diameter. To circumvent this problem, we used the Adobe Photoshop 5.0 program to assign to each focus a circle of 0.46 μm in diameter, representing the average diameter of fluorescent foci ($n = 60$). Thus, in Fig. 4, each focus was replaced with a computer-generated painted circle of constant diameter, centered around the central position of each fluorescent focus manually. Using this method, if the centers of two foci were closer than 0.46 μm, as demonstrated by the overlapping of the painted circles, the foci were considered to be coincident. If not, they were considered to be separate.

Table 2 shows the results of this analysis starting with the control (*oriC* versus LAdj). We observed 47% more *oriC* signals than LAdj signals (305 versus 207, respectively). This excess of *oriC* signals was probably a simple consequence of the close proximity of the *oriC* probe to the site of replication initiation. In any event, 26% of the *oriC* signals were coincident with an LAdj signal and 35% of the LAdj signals were coincident with an *oriC* signal. Because the painted foci occupy a significant fraction of the area of the cell, we estimated the frequency that any two foci would be found coincident by chance. By considering the fraction of cellular area occupied by each type of painted circle (see Materials and Methods), we estimated that 25% (compare to 26% observed) of the time an *oriC* signal would be found to coincide with an LAdj signal by chance and that 36% (compare to 35% observed) of the time an LAdj signal would be found to coincide with an *oriC* signal by chance. The similarity between the expected colocalization frequencies of randomly placed foci and experimentally determined colocalization frequencies is consistent with our interpretation that the relative positioning of the *oriC* and the LAdj regions is random.

Next, we analyzed the relative positioning of the TIR and the LAdj regions. We observed approximately equal numbers of TIR and LAdj signals ($n = 184$ and 177, respectively), which was expected for a chromosome configuration in which the two termini are held together. Most of the TIR and LAdj signals were found to colocalize: 86% of the TIR signals coincided with an LAdj signal, and 89% of the LAdj signals coincided with a TIR signal. The <100% colocalization was not surprising because the FISH staining frequency was not 100% as discussed previously. Thus, 86 and 89% colocalization frequencies observed are out of maximum possible observational values of 90 and 94%, respectively. Therefore, our data demonstrated that 95% of the time the two ends of the chromosomes were found to colocalize under the conditions used.

DISCUSSION

The genetic circularity of the *Streptomyces* chromosome was first demonstrated by conjugative mating experiments (13) and

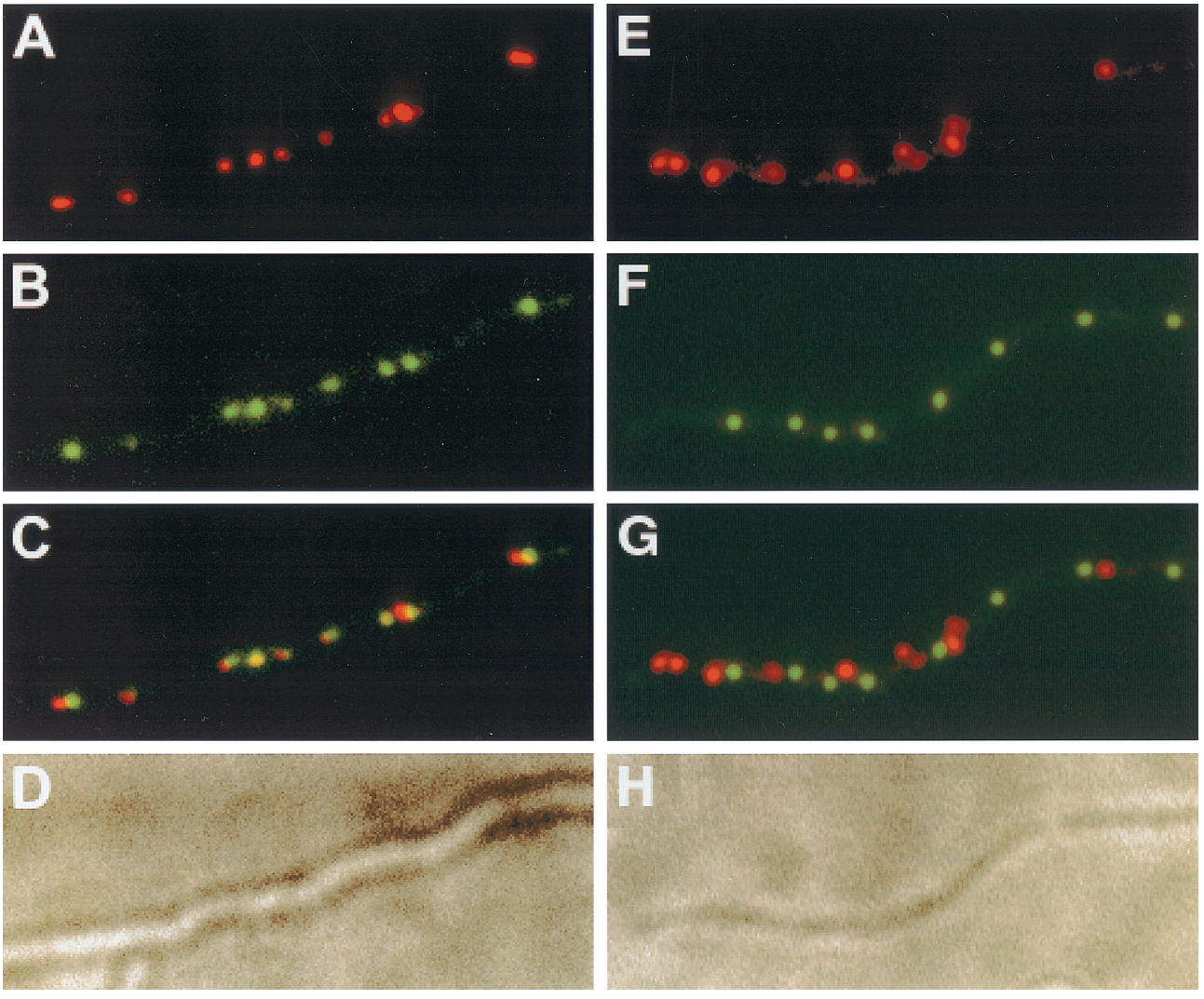

FIG. 3. (A to D) Dual-label FISH experiment showing the subcellular localizations of the TIRs and the LAdj region in *S. coelicolor* substrate mycelia. A Cy3-labeled TIR probe corresponding to both ends of the chromosome and a digoxigenin-labeled LAdj probe corresponding to a nonrepeated region adjacent to the left TIR were used to detect the localizations of the TIR and the LAdj regions in the same cells. (A) Fluorescent foci representing the localization of the TIR regions in cells; (B) fluorescent foci representing the localization of the LAdj region in cells; (C) overlay of panels A and B; (D) bright-field image showing the mycelium. (E to H) Dual-label FISH experiment showing the subcellular localizations of the *oriC* region and the LAdj region. A Cy3-labeled *oriC* probe corresponding to the replication origin regions and a digoxigenin-labeled LAdj probe corresponding to a nonrepeated region adjacent to the left TIR were used to detect the localizations of the *oriC* and the LAdj regions in the same cells. (E) Fluorescent foci representing the localization of the *oriC* region in cells; (F) fluorescent foci representing the localization of the LAdj region in cells; (G) overlay of panels A and B; (H) bright-field image showing the mycelium. Scale bar = 1 μm.

later confirmed by heteroclone and protoplast fusion experiments (14, 18). We now know, however, that the chromosome is a linear molecule with constant ends (24). How do we explain the apparent paradox between the genetic circularity and the physical linearity of the *Streptomyces* chromosome? One possible explanation proposed by Stahl and Steinberg (32) is that a linear genome gives rise to a circular genetic map if the genome is restricted to even numbers of crossovers. Wang et al. (34) tested the applicability of this explanation to the *Streptomyces* chromosome by carrying out plasmid-mediated interspecies matings and demonstrated a strong bias towards even numbers of crossovers. To explain the observed bias towards even numbers of crossovers, they proposed several hypotheses: the merozygotic nature of the conjugative mating process, the association of the chromosomal termini, the selective advantage conferred by the inheritance of telomeres from the same parent, and the homogenization of telomeres in the progeny. Wang et al. (34) discounted the last two hypotheses on the grounds that, in the matings performed, two of the progeny recovered were found to have inherited one telomere from each parent. These two progeny exhibited no growth disadvantage compared to that of their wild-type parents, and homogenization of the telomeres was not observed even after extensive subculturing.

Two possible explanations remained for the observed bias towards even numbers of crossovers: (i) the chromosome is linear and *Streptomyces* mating is merozygotic in nature and (ii) the chromosome adopts a circular configuration through

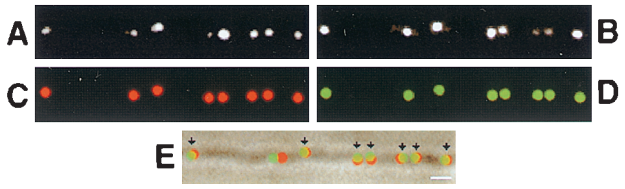

FIG. 4. Method for quantitative analysis of the relative positioning of various chromosomal sites. (A and B) Fluorescent foci representing the localizations of the TIR and the LAdj regions, respectively. (C and D) A computer-generated colored circle 0.46 μm in diameter was painted on top of each fluorescent focus centered around the central position of the focus to delineate an area considered the coincident range. Painting of the colored circles was performed entirely independently for each channel. (E) Overlay of the circles in panels C and D and bright-field image. If two different colored circles overlap, then they were considered coincident (arrows). Otherwise, they were considered separate. Scale bar = 1 μm.

the association of the termini. Conjugative matings in *Streptomyces* are merozygotic in nature; chromosome transfer from the donor to the recipient is incomplete. For complete haploid genomes to emerge, even numbers of crossovers would be required in recombination involving one partial and one complete chromosome, except when an end fragment is involved. If we assume that recombination involving end fragments is extremely rare, merozygosity may be able to explain the observed bias towards even numbers of crossovers even if the chromosome adopts a linear configuration in cells. Even numbers of crossovers would also be necessary for complete haploids to emerge if the chromosome ends associate and the chromosome adopts a circular configuration.

An additional observation, arising from the analysis of heteroclones, is the apparent transfer from the donor to the recipient of a linked segment of the genome spanning both ends of the chromosome. Heteroclones are merodiploid colonies that arise from a cross. The diploid region of a heteroclone behaves as a continuous segment of the genome. When the diploid regions from different classes of heteroclones were analyzed, they were found to overlap, covering the entire chromosome. In more than 10% of the heteroclones analyzed, the diploid regions were found to include both ends of the chromosome. Therefore, the hypothesis that *Streptomyces* chromosomes are linear molecules involved in merozygotic matings is not readily compatible with the results from the heteroclone experiments. A circular chromosome configuration, on the other hand, is compatible with the results of heteroclone analysis and with the observation of Wang et al. (34), regardless of whether the matings are merozygotic in nature. On balance,

TABLE 2. Coincident frequecies of the various chromosomal regions in *S. coelicolor* cells

Probes used	Region	% Separate[a]	% Coincident[a]	Total[b]
oriC and LAdj	*oriC*	74	26	305
	LAdj	65	35	207
TIR and LAdj	TIR	14	86	184
	LAdj	11	89	177

[a] Percentage of foci observed belonging to each class.
[b] Total number of foci observed from eight different fields of cells.

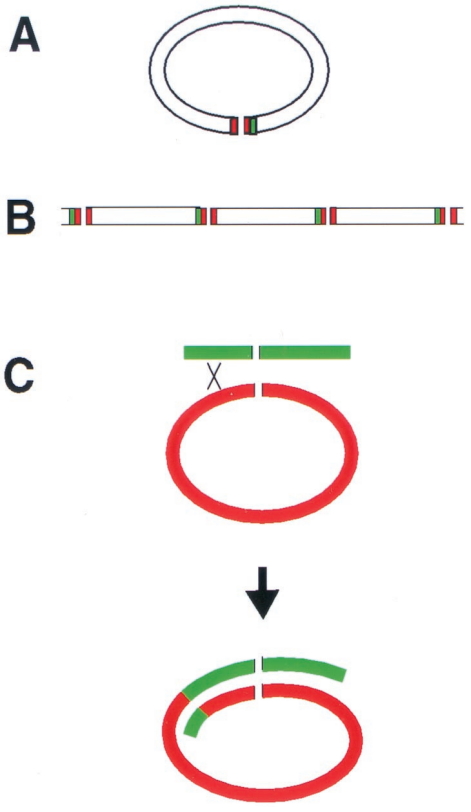

FIG. 5. Models for chromosome configuration. A circular configuration (A) and an end-to-end-linked chromosome configuration (B) are shown. Green represents the LAdj region, and red represents the TIR regions. (C) Model for the generation of a heteroclone chromosome as a result of recombination with a circular chromosome as proposed by Hopwood (15).

then, the simplest explanation for the genetic circularity of the chromosome is that the chromosome adopts a circular configuration through the association of the termini.

The goal of the present work was to test this hypothesis cytologically. To determine whether the *Streptomyces* chromosome assumes a linear or circular configuration in cells, we performed FISH experiments determining the locations of the origin of replication region (*oriC*), the ends of the chromosome (TIRs), and a region of the chromosome adjacent to but outside of the left TIR (LAdj). Our principal findings are that the ends of the chromosomes (TIRs) and the LAdj region colocalize in an approximately 1:1 ratio but that the *oriC* region and the LAdj regions of the chromosome do not to colocalize, hereby demonstrating that the ends of the *Streptomyces* chromosome associate in cells. The association of the chromosomal termini is consistent with a circular chromosome configuration (Fig. 5A). A circular chromosome configuration is compatible with the heteroclone chromosome structure previously proposed by Hopwood (15) (Fig. 5C). It should be noted, however, that our FISH data, considered alone, are also consistent with a model in which linear chromosomes are linked to each other in an end-to-end configuration (Fig. 5B). However, it is difficult to imagine how this chromosome configuration would be compatible with the existence of heteroclones. We therefore favor the hypothesis that the linear *Streptomyces* chromosome adopts

a circular configuration in cells through the association of the chromosomal termini.

What is the mechanism responsible for holding the ends of the *Streptomyces* chromosome together? To date, two types of chromosome ends have been described for linear prokaryotic replicons: those consisting of covalently closed hairpin loops without bound proteins as found in *Borrelia* chromosomes and linear plasmids (2, 4) and those consisting of inverted repeats with covalently attached 5′-terminal proteins as found in all characterized *Streptomyces* chromosomes and linear plasmids (7, 20, 24). Other linear replicons sharing the same characteristics as those of the linear *Streptomyces* replicons include the genomes of certain bacteriophages (e.g., *Bacillus subtilis* ϕ29, *Escherichia coli* PRD1, and *Streptococcus pneumoniae* HB-3), the mammalian adenoviruses, and the linear plasmids of plant and fungal mitochondria (12). The identity of the 5′-terminal protein of *Streptomyces* chromosomes is still unknown. In bacteriophages and adenoviruses, the genes for the 5′-terminal proteins have been cloned and the proteins have been shown to play an essential role in viral DNA replication.

Intriguingly, the circular form of viral DNA molecules had been found previously in DNA preparations from both ϕ29 and adenoviruses (27, 29). It has been suggested that a protein factor is responsible for the formation and the maintenance of the circular form (27, 29). The circular configuration observed for the *Streptomyces* linear chromosomes is most likely achieved by the presence of a protein(s) that is capable of holding the ends of the chromosome together, as previously suggested in a number of reports (8, 16, 30). The identities of the 5′-terminal proteins found on *Streptomyces* linear plasmids and chromosomes are currently unknown. Whether the 5′-terminal protein plays a role in the association of the two chromosomal ends in *Streptomyces* remains to be determined.

ACKNOWLEDGMENTS

This work was supported by a grant from the National Science Foundation (MCB-9727234).

We thank K. Chater and Amy Gehring for helpful advice.

ADDENDUM IN PROOF

A recent report describes the cloning of the gene for the 5′ terminal protein of the *Streptomyces* chromosome (K. Bao and S. N. Cohen, Genes Dev. **15:**1518–1527, 2001).

REFERENCES

1. **Allardet-Servent, A., S. Michaux-Charachon, E. Jumas-Bilak, L. Karayan, and M. Ramuz.** 1993. Presence of one linear and one circular chromosome in the *Agrobacterium tumefaciens* C58 genome. J. Bacteriol. **175:**7869–7874.
2. **Barbour, A. G., and C. F. Garon.** 1987. Linear plasmids of the bacterium *Borrelia burgdorferi* have covalently closed ends. Science **237:**409–411.
3. **Casjens, S., and W. M. Huang.** 1993. Linear chromosomal physical and genetic map of *Borrelia burgdorferi*, the Lyme disease agent. Mol. Microbiol. **8:**967–980.
4. **Casjens, S., M. Murphy, M. DeLange, L. Sampson, R. van Vugt, and W. M. Huang.** 1997. Telomeres of the linear chromosomes of Lyme disease spirochaetes: nucleotide sequence and possible exchange with linear plasmid telomeres. Mol. Microbiol. **26:**581–596.
5. **Chater, K. F.** 2000. Developmental decisions during sporulation in the aerial mycelium in *Streptomyces*, p. 33–48. *In* Y. V. Brun and L. J. Shimkets (ed.), Prokaryotic development. American Society for Microbiology, Washington, D.C.
6. **Chater, K. F., and D. A. Hopwood.** 1973. Differentiation in actinomycetes, p. 143–160. *In* J. M. Ashworth and J. E. Smith (ed.), Microbial differentiation. Society for General Microbiology Symposium 23. Cambridge University Press, Cambridge, United Kingdom.
7. **Chen, C. W.** 1996. Complications and implications of linear bacterial chromosomes. Trends Genet. **12:**192–196.
8. **Chen, C. W., Y.-S. Lin, Y.-L. Yang, M.-F. Tsu, H.-M. Chang, H. M. Keiser, and D. A. Hopwood.** 1994. The linear chromosome of Streptomyces: structure and dynamics. Actinomycetologica **8:**103–112.
9. **Ferdows, M. S., and A. G. Barbour.** 1989. Megabase-sized linear DNA in the bacterium *Borrelia burgdorferi*, the Lyme disease agent. Proc. Natl. Acad. Sci. USA **86:**5969–5973.
10. **Gordon, G. S., D. Sitnikov, C. D. Webb, A. Teleman, A. Straight, R. Losick, A. W. Murray, and A. Wright.** 1997. Chromosome and low copy plasmid segregation in *E. coli*: visual evidence for distinct mechanisms. Cell **90:**1113–1121.
11. **Gray, D. I., G. W. Gooday, and J. I. Prosser.** 1990. Apical hyphal extension in *Streptomyces coelicolor* A3(2). J. Gen. Microbiol. **136:**1077–1084.
12. **Hinnebusch, J., and K. Tilly.** 1993. Linear plasmids and chromosomes in bacteria. Mol. Microbiol. **10:**917–922.
13. **Hopwood, D. A.** 1965. A circular linkage map in the actinomycete *Streptomyces coelicolor*. J. Mol. Biol. **12:**514–516.
14. **Hopwood, D. A.** 1966. Lack of constant genome ends in *Streptomyces coelicolor*. Genetics **54:**1177–1184.
15. **Hopwood, D. A.** 1967. Genetic analysis and genome structure in *Streptomyces coelicolor*. Bacteriol. Rev. **31:**373–403.
16. **Hopwood, D. A.** 1997. Delving into the *Streptomyces* chromosome. Dev. Ind. Microbiol. **34:**1–6.
17. **Hopwood, D. A.** 1999. Forty years of genetics with *Streptomyces*: from *in vivo* through *in vitro* to *in silico*. Microbiology **145:**2183–2202.
18. **Hopwood, D. A., and H. M. Wright.** 1978. Bacterial protoplast fusion: recombination in fused protoplasts of *Streptomyces coelicolor*. Mol. Gen. Genet. **162:**307–317.
19. **Hopwood, D. A., M. J. Bibb, K. F. Chater, T. Kieser, C. J. Bruton, H. M. Kieser, D. J. Lydiate, C. P. Smith, J. M. Ward, and H. Schrempf.** 1985. Genetic manipulation of Streptomyces: a laboratory manual. The John Innes Foundation, Norwich, United Kingdom.
20. **Huang, C. H., Y. S. Lin, Y. L. Yang, S. W. Huang, and C. W. Chen.** 1998. The telomeres of *Streptomyces* chromosomes contain conserved palindromic sequences with potential to form complex secondary structures. Mol. Microbiol. **28:**905–916.
21. **Ikeda, H., E. T. Seno, C. J. Bruton, and K. T. Chater.** 1984. Genetic mapping, cloning and physiological aspects of the glucose kinase gene of *Streptomyces coelicolor*. Mol. Gen. Genet. **196:**501–507.
22. **Jensen, R. B., and L. Shapiro.** 1999. The *Caulobacter crescentus* smc gene is required for cell cycle progression and chromosome segregation. Proc. Natl. Acad. Sci. USA **96:**10661–10666.
23. **LeBlond, P., M. Redenback, and J. Cullum.** 1993. Physical map of the *Streptomyces lividans* 66 genome and comparison with that of the related strain *Streptomyces coelicolor* A3(2). J. Bacteriol. **175:**3422–3429.
24. **Lin, Y. S., H. M. Kieser, D. A. Hopwood, and C. W. Chen.** 1993. The chromosomal DNA of *Streptomyces lividans* 66 is linear. Mol. Microbiol. **10:**923–933.
25. **Musialowski, M. S., F. Flett, G. B. Scott, G. Hobbs, C. P. Smith, and S. G. Oliver.** 1994. Functional evidence that the principal DNA replication origin of the *Streptomyces coelicolor* chromosome is close to the *dnaA-gyrB* region. J. Bacteriol. **176:**5123–5125.
26. **Niki, H., and S. Hiraga.** 1998. Polar localization of the replication origin and terminus in *Escherichia coli* nucleoids during chromosome partitioning. Genes Dev. **12:**1036–1045.
27. **Ortin, J., E. Vinuela, M. Salas, and C. Vasquez.** 1971. DNA-protein complex in circular DNA from phage phi-29. Nat. New Biol. **234:**275–277.
28. **Reeves, A. R., D. A. Post, and T. J. Vanden Boom.** 1998. Physical-genetic map of the erythromycin-producing organism *Saccharopolyspora erythraea*. Microbiology **144:**2151–2159.
29. **Robinson, A. J., H. B. Younghusband, and A. J. D. Bellett.** 1973. A circular DNA-protein complex from adenoviruses. Virology **56:**54–69.
30. **Sakaguchi, K.** 1990. Invertrons, a class of structurally and functionally related genetic elements that includes linear DNA plasmids, transposable elements, and genomes of adeno-type viruses. Microbiol. Rev. **54:**66–74.
31. **Schwedock, J., J. R. McCormick, E. R. Angert, J. R. Nodwell, and R. Losick.** 1997. Assembly of the cell division protein FtsZ into ladder-like structures in the aerial hyphae of *Streptomyces coelicolor*. Mol. Microbiol. **25:**847–858.
32. **Stahl, F. W., and C. M. Steinberg.** 1964. The theory of formal phage genetics for circular maps. Genetics **50:**531–538.
33. **Streisinger, G., R. S. Edgar, and G. H. Denhardt.** 1964. Chromosome structure in phage T4, I. Circularity of the linkage map. Proc. Natl. Acad. Sci. USA **51:**775–779.
34. **Wang, S. J., H. M. Chang, Y. S. Lin, C. H. Huang, and C. W. Chen.** 1999. *Streptomyces* genomes: circular genetic maps from the linear chromosomes. Microbiology **145:**2209–2220.
35. **Webb, C. D., A. Teleman, S. Gordon, A. Straight, A. Belmont, D. C. Lin, A. D. Grossman, A. Wright, and R. Losick.** 1997. Bipolar localization of the replication origin regions of chromosomes in vegetative and sporulating cells of *B. subtilis*. Cell **88:**667–674.
36. **Willems, H., C. Jager, and G. Baljer.** 1998. Physical and genetic map of the obligate intracellular bacterium *Coxiella burnetii*. J. Bacteriol. **180:**3816–3822.